ANALYSIS OF PROSEDS BARE-TETHER PERFORMANCE

J.R.Sanmartín

Universidad Politécnica de Madrid, Spain

E.C.Lorenzini and M.L.Cosmo

Harvard-Smithsonian Center for Astrophysics, Cambridge, MA, USA

R.D.Estes

OnScreen Science, Inc., Cambridge, MA, USA

Abstract

NASA's tether experiment ProSEDS will be placed in orbit on board a Delta-II rocket in early 2003. ProSEDS will test bare-tether electron collection, deorbiting of the rocket second stage, and the system dynamic stability. ProSEDS performance will vary both because ambient conditions change along the orbit and because tether-circuit parameters follow a step by step sequence in the current operating cycle. In this work we discuss how measurements of tether current and bias, plasma density, and deorbiting rate can be used to check the OML law for current collection. We review circuit bulk elements; characteristic lengths and energies that determine collection (tether radius, electron thermal gyroradius and Debye length, particle temperatures, tether bias, ion ram energy); and lengths determining current and bias profiles along the tether (extent of magnetic self-field, a length gauging ohmic versus collection impedances, tether length). The analysis serves the purpose of estimating ProSEDS behavior in orbit and fostering our ability for extrapolating ProSEDS flight data to different tether and environmental conditions.

1. Introduction

NASA's Propulsive Small Expendable Deployer System (ProSEDS) will demonstrate propulsion by a bare electrodynamic tether. ProSEDS will fly as secondary payload on a Delta II rocket and will be deployed upwards from its second stage in a 360 km nearly circular orbit at an inclination of 36°. The geomagnetic field will both induce an electric field on the orbiting tether and exert a dragging force on the resulting current. This will strongly increase the decay rate of the Delta stage. The launch date of ProSEDS is now scheduled for early 2003.[1]

The ProSEDS tether is about 15 km long. The 10 km (10,132 m) segment first deployed is a nonconductive Dyneema tape of average cross-section 1.2 mm × 0.2 mm, with a 20 m leader made of Kevlar, total weight being about 1.5 kg. Following the tape is a 5 km (5,080 m) Al wire of 1.2 mm diameter, left bare except for its last 215 m, which are insulated with overbraided Kevlar; total weight is 10 kg. The bare segment has a C-COR coating that modifies optical properties for passive control of wire temperature and protects aluminum against atomic oxygen. The Delta second stage has a mass of 994 kg, while the body attached to the other end of the tether for stability purposes has a 21.4 kg mass.

Electrons are collected over some upper portion of the bare wire that will come out positively biased with respect to the surrounding plasma. The full electron current collected is reemitted into the ionosphere by an active hollow-cathode device at the Delta stage. The Hollow Cathode will keep the platform at less than 30 V of the local plasma potential. Estimated average currents, depending on ambient conditions, are 1.3 - 1.4 A with about 3.5 A peak values, corresponding drag being 0.15 N and 0.4 N respectively. Part of the energy taken from the orbital motion will be used to recharge batteries that might allow for extended measurements, using, in particular, Langmuir probes and a differential-ion-flux probe. ProSEDS current is run under two different types of operation. An orbit-decay rate of about 11 km/day is expected for the first 5 orbits, covering the first type, and about 19 km/day for the remaining orbits.

2. ProSEDS current-collection regime

Dimensionless parameters characterizing the magnetized ionospheric plasma at LEO altitudes are an ion-to-electron temperature ratio (*i*) about unity and a small ratio of Debye length to electron thermal-gyroradius (*ii*). The orbiting tether introduces new parameters: small ratios (tether radius / Debye length) (*iii*) and (ion ram energy/ $e\Delta V$) (*iv*), and a large ion Mach number (*v*).

Here ΔV is tether bias relative to the ionosphere, which is of the order of the full induced electromotive force, $\varepsilon_{ind} = E_m L_t$, where $L_t \approx 5$ km is the *conductive* tether length and E_m is the motional electric field (product of orbiting speed and geomagnetic-field component perpendicular to the orbital plane). Simulations indicate that the tether stays straight and vertical during the full first day in orbit, particularly over the early five orbits that will be of interest here. Figure 1 shows expected values for ε_{ind} from a particular numerical simulation of the ProSEDS orbital evolution.[2]

Based on the small values of ratios (*ii*) - (*iv*), current collection by unit length of ProSEDS bare-tether is expected to follow the orbital-motion-limited (OML) law, which is just proportional to $N_\infty p\sqrt{\Delta V}$, where N_∞ is ambient plasma density and p is perimeter of tether cross-section.[3] ProSEDS will particularly serve to test in space whether ram effects on ions due to the large ion Mach number (parameter *v*), or even geomagnetic effects on electrons (parameter *ii*), could invalidate the OML law.

The variations along tether length of bias ΔV and current I flowing in the tether, introduce a new, fundamental number characterizing current and bias profiles,

$$\frac{L_t}{L^*} \equiv l_t \approx 4.17 \times \left(\frac{500V}{\varepsilon_{ind}} \right)^{1/3} \times \left(\frac{R_t}{250\,\Omega} \times \frac{N_\infty}{10^{12}\, m^{-3}} \right)^{2/3}, \qquad (1)$$

where R_t is tether resistance. The conductive segment of ProSEDS has perimeter $p = \pi \times 1.2$ mm and is made of aluminum strands; the effective conductive cross-section area A_c was found to result in a resistance

$$R_t \equiv L_t/\sigma A_c = 250\ \Omega \text{ at } 20\ ^\circ\text{C}, \qquad (\sigma \equiv \text{Al conductivity}).$$

The length L^* in Eq.(1) gauges ohmic versus OML-collection impedance, and is defined by

$$L^* \times eN_\infty \times \frac{p}{\pi} \sqrt{\frac{2eE_m L^*}{m_e}} = \frac{3}{4} \sigma A_c E_m \equiv \frac{3}{4} \frac{\varepsilon_{ind}}{R_t}.$$

Figures 2-4 show R_t, N_∞, and l_t for the same simulations of Fig. 1. Effects of the magnetic self-field are weaker the smaller a parameter proportional to $(A_c^2 p)^{1/3}$, and are fully negligible for our thin wire.[4]

3. Current and bias at cathodic end of tether

The ProSEDS current is run under two different operating cycles. Primary cycles with period 60 s (Fig.5) start at Delta Time = 12,666 seconds and run for 5 orbits. The tether is in *open circuit mode* (Hollow Cathode disconnected from tether, making it to float electrically) for the first 35 s, with the HC *idle* during 30 s and *on* during the remaining 5 s. For the rest of each cycle the tether is connected to the HC, running in a *resistor* mode (with a $Z_\Omega = 2.32$ kΩ load in the circuit) for 5 seconds, and in *shunt* mode (tether current shorted to the HC) in the final 20 s. For the currents of interest the Hollow Cathode may be characterized by a negative resistance $r_{HC} = -4\ \Omega$ and a limit potential drop at low current $\Phi_{HC} = 40$ V.

The secondary operating cycle that is activated after 5 orbits has a period of 80 seconds (Fig.6). The tether runs in the *shunt* mode for the first 30 s and in a *battery* mode for the rest of the cycle. The battery has

negligible internal resistance and an electromotive force $\varepsilon_{bat} = 120$ V. From Figs. 1, 2 we have $|r_{HC}| << R_t << Z_\Omega$ and $\Phi_{HC} < \varepsilon_{bat} << \varepsilon_{ind}$.

Whichever bulk elements at the cathodic end C of the tether, bias ΔV relative to the plasma varies along tether length due to both ohmic and induced electric-field drops,

$$\frac{d\Delta V}{ds} = \frac{I(s)}{\sigma A_C} - E_m , \qquad (2)$$

with s running from anodic top A to bottom C (Fig.7). Over a segment AB with $\Delta V > 0$, electrons are collected at the rate given by the OML law,

$$\frac{dI}{ds} = eN_\infty \times \frac{p}{\pi} \times \sqrt{\frac{2e\Delta V(s)}{m_e}} . \qquad (3)$$

Equations (2), (3) are readily integrated, with results conveniently displayed in dimensionless variables[4]

$$i \equiv I / \sigma A_c E_m \ \ (< 1), \qquad \varphi \equiv \Delta V / E_m L^*, \qquad l \equiv s / L^*. \qquad (4)$$

One finds $\varphi^{3/2} + 2i - i^2 = constant$ and (using conditions $i_A = \varphi_B = 0$)

$$\varphi_A^{3/2} = 2i_B - i_B^2, \qquad (5)$$

$$\frac{length\ AB}{L^*} \equiv l_B = \int_0^{\varphi_A(i_B)} \frac{d\varphi}{\sqrt{(1 - i_B)^2 + \varphi^{3/2}}}, \qquad (6)$$

with $l_B(i_B) \approx (2i_B)^{2/3}$ at small i_B and $l_B(1) = 4$.

Ions are collected over the segment BC with $\Delta V < 0$ according to the OML law too, at a rate $\mu \equiv \sqrt{m_e/m_i}$ times smaller,

$$\frac{dI}{ds} = -\mu \times eN_\infty \times \frac{p}{\pi} \sqrt{\frac{2e|\Delta V|}{m_e}} . \qquad (3')$$

From Eqs. (2) and (3') one readily obtains $\mu |\varphi|^{3/2} + 2i - i^2 = constant$, and using condition $\varphi_B = 0$,

$$\mu |\varphi_C|^{3/2} + 2i_C - i_C^2 = 2i_B - i_B^2, \qquad (7)$$

$$l_t - l_B(i_B) = \int_0^{|\varphi_C|} \frac{d|\varphi|}{1 - i} \equiv \int_0^{|\varphi_C|} \frac{d|\varphi|}{\sqrt{(1 - i_B)^2 + \mu |\varphi|^{3/2}}} . \qquad (8)$$

For $\mu \approx 1/170$ (oxygen ions) and values of l_t as shown in Fig.4, $\mu l_t^{3/2}$ is small. Since we clearly have $l_t > |\varphi_C|$ we also have $\mu |\varphi_C|^{3/2}$ small. With $l_B(i_B)$ given by Eqs.(5) and (6), Eqs. (7, 8) determine a relation between i_C and $|\varphi_C|$, that is, between current and bias at tether end C.

A second equation for i_C and $|\varphi_C|$ is provided by the circuit relation for the bulk element at C, which is different for each different mode:

3a) Open circuit mode. Here we have

$$i_C = 0. \tag{9}$$

Equation (7) then proves i_B small, and leads to $l_B \approx \varphi_A \approx \mu^{2/3}|\varphi_C|$ in Eqs. (5, 6). Equation (8) now takes the approximate form

$$l_t \approx |\varphi_C| \times [1 + 0.3\mu\,|\varphi_C|^{3/2} + \mu^{2/3}], \tag{10}$$

proving $|\varphi_C|$ close to l_t. One easily shows that our having ignored the insulation over a short segment of the tether above bottom C results in corrections to Eq.(10) that are of order higher than $\mu\,|\varphi_C|^{3/2}$ and $\mu^{2/3}$.

3b) Resistor mode. Current at C now satisfies the relation

$$|\varphi_C| = \frac{\Phi_{HC} + (r_{HC} + Z_\Omega) I_C}{E_m L^*} \approx l_t \times \left[\frac{\Phi_{HC}}{\varepsilon_{ind}} + \frac{Z_\Omega}{R_t}\, i_C\right], \tag{9'}$$

with the r_{HC} term negligible. Since Z_Ω / R_t is large, the current i_C must be small, again implying small i_B, here leading to $l_B \approx \varphi_A \approx (\mu|\varphi_C|^{3/2} + 2i_C)^{2/3}$. Equation (8) now takes the form

$$l_t \approx |\varphi_C| \times [1 + 0.3\mu\,|\varphi_C|^{3/2} + (\mu + 2i_C/|\varphi_C|^{3/2})^{2/3} + i_C], \tag{10'}$$

with $|\varphi_C|$ again close to l_t, and $i_C \approx R_t / Z_\Omega$, to lowest order, in Eq. (9').

3c) Shunt mode. Here we have

$$\frac{|\varphi_C|}{l_t} = \frac{\Phi_{HC} + r_{HC} I_C}{\varepsilon_{ind}} \equiv \frac{\Phi_{HC}}{\varepsilon_{ind}} + \frac{r_{HC}}{R_t} i_C, \tag{9''}$$

$|\varphi_C|$ now being small against l_t. One may verify in Eqs. (8) and (9'') that, for l_t moderately large at most (l_t less than about 7 in Fig.4), current and bias at C satisfy $(1 - i_C)^2 \approx (1 - i_B)^2 >> \mu\,|\varphi_C|^{3/2}$. Then, one may write Eq.(8), using (7), as

$$\frac{l_B(i_B)}{l_t} \approx 1 - \frac{|\varphi_C|/l_t}{1 - i_C} \times \left[1 + \frac{3}{10}\,\frac{\mu\,|\varphi_C|^{3/2}}{(1 - i_C)^2}\right]. \tag{10''}$$

With i_B taken from Eq.(7) simplified to the form $i_B = i_C + \mu\,|\varphi_C|^{3/2} / 2(1 - i_C)$, we may write $l_B(i_B)$ on the left-hand-side of (10'') in terms of i_C and φ_C,

$$l_B(i_B) \approx l_B(i_C) + \frac{\mu\,|\varphi_C|^{3/2}}{2(1 - i_C)} \times \frac{dl_B}{di_C}.$$

Note that equations for the *shunt* mode would apply to the *battery* mode with just the change $\Phi_{HC} \rightarrow 4\Phi_{HC}$.

Equations (9-10") show how current and bias at tether end C may be predicted (if OML current-collection is valid) once ambient conditions and tether parameters are known, and the bulk element at C is defined. Those equations determine i_C and $|\varphi_C|$ for the *open-circuit, resistor*, and *shunt* modes. Then one just writes $I_C = i_C \times \varepsilon_{ind} / R_t$ and $|\Delta V_C| = |\varphi_C| \times E_m L^*$.

4. Tests of OML current collection from ProSEDS primary-cycle data

4a) Plasma density measurements.

Equations (9-10") can be considered in a reverse way: Values of current I_C and bias ΔV_C, if measured, could be used to determine a number of actual ambient and tether conditions. This may serve as a test of the validity of the OML law for current-collection.

Equation (1) for the dimensionless length l_t can be rewritten as an equation for the plasma density,

$$\frac{N_\infty}{10^{12}\ m^{-3}} \approx \frac{250\,\Omega}{R_t} \times \left(\frac{\varepsilon_{ind}}{500 V}\right)^{1/2} \times \left(\frac{l_t}{4.17}\right)^{3/2} . \qquad (1')$$

Measuring ΔV_C during the *open-circuit* mode, and I_C during the *resistor* and the *shunt* modes of a primary cycle could in principle determine all three quantities ε_{ind}, R_t, and l_t, yielding N_∞ in (1'). Direct measurement of plasma density during primary cycles using a Langmuir probe will yield an independent value for N_∞, to be compared with (1').

There are about 450 primary cycles, each cycle providing, in principle, a test of the OML law. Note that, as shown in Figs. 1-4, variations of ε_{ind}, R_t, N_∞, and l_t are expected to cover a large parametric domain; this will result in very broad testing. On the other hand we may safely assume that tether temperature (and thus tether resistance R_t), and both plasma density N_∞ and motional electric field E_m, leading to the length ratio l_t, change negligibly during a cycle (60 s, or about 450 km), except possibly when crossing the terminator.

It turns out, however, that ΔV_C in the *open-circuit* mode, and I_C in the *resistor* mode, both basically determine the induced electromotive force ε_{ind}. One would find $\varepsilon_{ind} \approx |\Delta V_C|$ (*open circuit*) from Eq.(10) and $\varepsilon_{ind} \approx Z_\Omega \times I_C$ (*resistor*) from Eqs.(9'-10'). This has a positive side, because measuring ΔV_C in the *open-circuit* mode is problematic. (Intended direct measurements of the motional electric field using a

magnetometer present uncertainties too.) On the other hand, it then becomes impossible to obtain both R_t and l_t, for use in Eq.(1'), from the single remaining measurement of I_C in the *shunt* mode.

Fortunately, tether temperature is basically governed by solar irradiation, and is weakly affected by Joule heating, or heating arising from the impact of the attracted particles. As a result, there may be no need for measuring tether resistance, which could be quite reasonably predicted from ProSEDS orbital position at the particular cycle considered, independently from actual ionospheric conditions.

Equations (9-10), Eqs. (9'-10'), and (9"-10"), yield, respectively,

$$\varepsilon_{ind} \approx |\Delta V_C|^{oc} \times [1 + 0.3\,\mu\, l_t^{3/2} + \mu^{2/3}], \tag{11}$$

$$\varepsilon_{ind} \approx \left[Z_\Omega \left(1 + \frac{R_t}{Z_\Omega} \right) I_C{}^{res} + \Phi_{HC} \right] \times \left[1 + 0.3\,\mu\, l_t{}^{3/2} + \left(\mu + \frac{2}{l_t{}^{3/2}} \times \frac{R_t}{Z_\Omega} \right)^{2/3} \right], \tag{12}$$

and

$$1 - \frac{1}{1 - i_C} \times \frac{|\varphi_C|}{l_t} \times \left[1 + \frac{0.3\,\mu\, l_t{}^{3/2}}{(1 - i_C)^2} \times \left(\frac{|\varphi_C|}{l_t} \right)^{3/2} \right] =$$

$$= \frac{l_B(i_C)}{l_t} \times \left[1 + \frac{\mu\, l_t{}^{3/2} \times dl_B / i_C}{2(1 - i_C) \times l_B(i_C)} \times \left(\frac{|\varphi_C|}{l_t} \right)^{3/2} \right]. \tag{13}$$

In Eq. (13), $l_B(i_C)$ is obtained by setting $i_B \to i_C$ in (5) and (6), and auxiliary relations

$$i_C \equiv I_C{}^{sh} \times \frac{R_t}{\varepsilon_{ind}}, \qquad \frac{|\varphi_C|}{l_t} \equiv \frac{\Phi_{HC} + r_{HC}\, I_C{}^{sh}}{\varepsilon_{ind}}, \tag{14a, b}$$

are used. Assuming R_t known from the orbital position, one might ignore Eq. (11) and introduce measured values $I_C{}^{res}$ and $I_C{}^{sh}$ in Eqs. (12)-(14a, b) to determine ε_{ind} and l_t.

4b) Deorbiting rate measurements.

A second test on OML collection is provided by the rate of orbital decay, which is dependent on the magnetic-drag power. At any given time, this power is proportional to the average tether current,

$$W = Orbital\ Speed \times Drag = \varepsilon_{ind}\, \tilde{I}, \qquad \tilde{I} \equiv \int_0^{L_t} I(s)\, ds / L_t\ .$$

From Eq. (2) one readily finds $\tilde{I} / \sigma A_C = E_m + (\Delta V_C - \Delta V_A) / L_t$, leading to

$$\frac{R_t\, W}{\varepsilon_{ind}{}^2} = 1 - \left[\frac{|\varphi_C|}{l_t} + \frac{\varphi_A}{l_t} \right]. \tag{15}$$

Results on φ_A and $|\varphi_C|$ in Sec.3 for the *open-circuit* and *resistor* modes immediately yield

$$\frac{R_t W_{oc}}{\varepsilon_{ind}^2} \approx 0.3\,\mu\, l_t^{3/2}, \tag{16a}$$

$$\frac{R_t W_{res}}{\varepsilon_{ind}^2} \approx 0.3\,\mu\, l_t^{3/2} + \frac{R_t}{Z_\Omega}, \tag{16b}$$

respectively. In the *shunt* mode we have $|\varphi_C| / l_t$ small. We may then use Eqs. (5) and (7) to write, to lowest order, $\varphi_A \approx (2i_C - i_C^2)^{2/3}$, yielding

$$\frac{R_t W_{sh}}{\varepsilon_{ind}^2} \approx 1 - \left[\frac{\Phi_{HC}}{\varepsilon_{ind}} + \frac{r_{HC}}{R_t} i_C + \frac{\left(2i_C - i_C^2\right)^{2/3}}{l_t}\right]. \tag{16c}$$

The average drag-power over a full primary cycle would then be

$$W_{av}(primary) = \frac{7}{12} W_{oc} + \frac{1}{12} W_{res} + \frac{1}{3} W_{sh} \approx$$

$$\frac{\varepsilon_{ind}^2}{3R_t} \times \left[1 - \frac{\Phi_{HC} + r_{HC} I_C^{sh}}{\varepsilon_{ind}} - \frac{\left(2\varepsilon_{ind} - R_t I_C^{sh}\right)^{2/3} \left(R_t I_C^{sh}\right)^{2/3}}{l_t\, \varepsilon_{ind}^{4/3}} + 0.6\,\mu\, l_t^{3/2} + \frac{R_t}{4Z_\Omega}\right]. \tag{17}$$

In Equation (17), I_C^{sh}, and R_t, $\varepsilon_{\rm ind}$ and l_t are measured or determined as discussed in Sec. 4b. Results from (17) would be compared to values obtained from actual measurements of orbital decay.

5. Conclusions

Measurements of tether current at cathodic end, plasma density, and deorbiting rate during the first 5 orbits can be used for a check of the OML current-collection law under a variety of conditions.

References

1. L. Johnson, R. D. Estes, E. C. Lorenzini, M. Martínez-Sánchez and J. R. Sanmartín, *J. Spacecraft and Rockets* **37**, 173 (2000).

2. E. C. Lorenzini, *Annual report* # 3, NASA Grant NAG8-1605 (July 2002).

3. J. R. Sanmartín and R. D. Estes, *Physics of Plasmas* **6**, 395 (1999) and **8**, 4234 (2001); R. D. Estes and J. R. Sanmartín, *Physics of Plasmas* **7**, 4320 (2000).

4. J. R. Sanmartín and R. D. Estes, *Journal of Geophysical Research* (in press).

Figure legends

Fig.1 Electromotive force from simulation results for Summer 2002 launch; nominal solar condition.

Fig.2 Tether resistance from the same simulations of Fig.1.

Fig.3 Plasma density from the same simulations of Fig.1.

Fig.4 Length ratio l_t as given in Eq.(1) and derived from the results of Figs.1-3.

Fig.5 First operating cycle: modes *open circuit* (1a *plasma contactor idle*, 1b *contactor on*);

shunt (2); *resistor* (3).

Fig.6 Second operating cycle: modes *shunt* (2) and *battery charge* (4).

Fig.7 Voltage diagram. A bulk element at cathodic end C relates current and bias there.

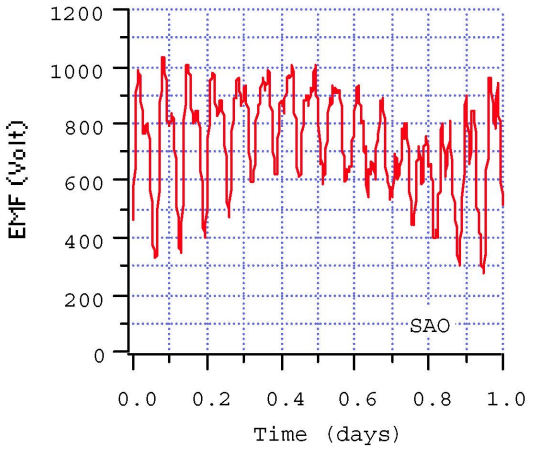

Figure 1

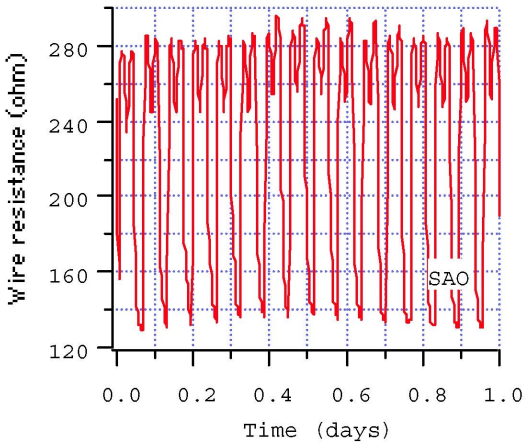

Figure 2

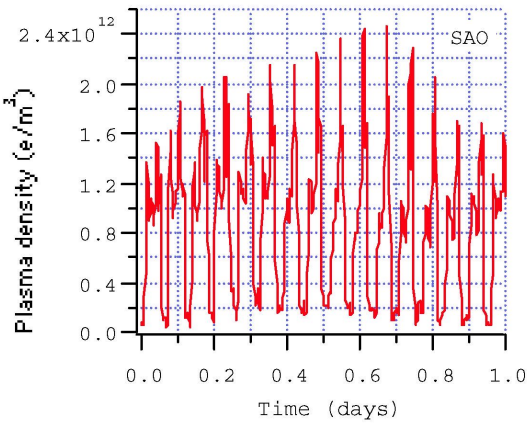

Figure 3

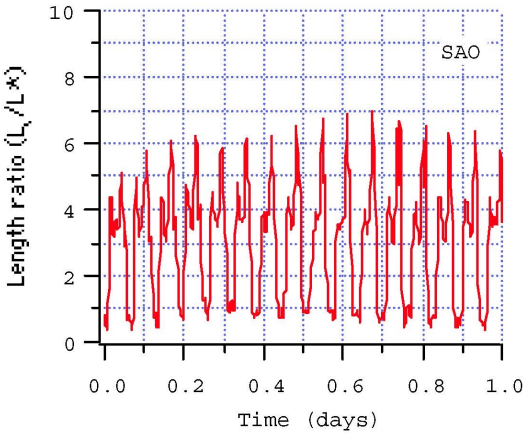

Figure 4

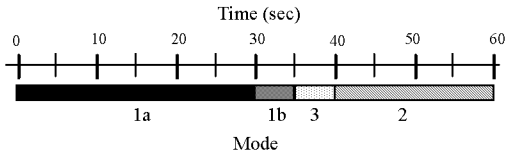

Figure 5 Operating cycle #1 (60-sec cycle)

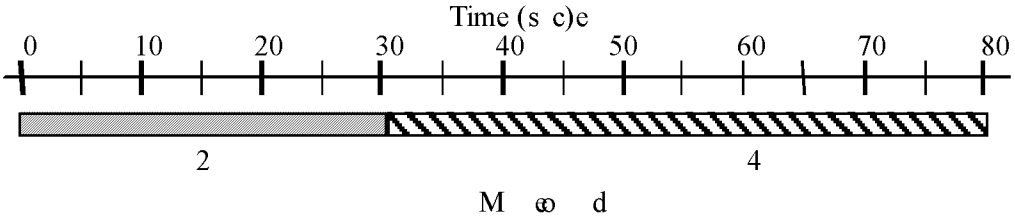

Figure 6

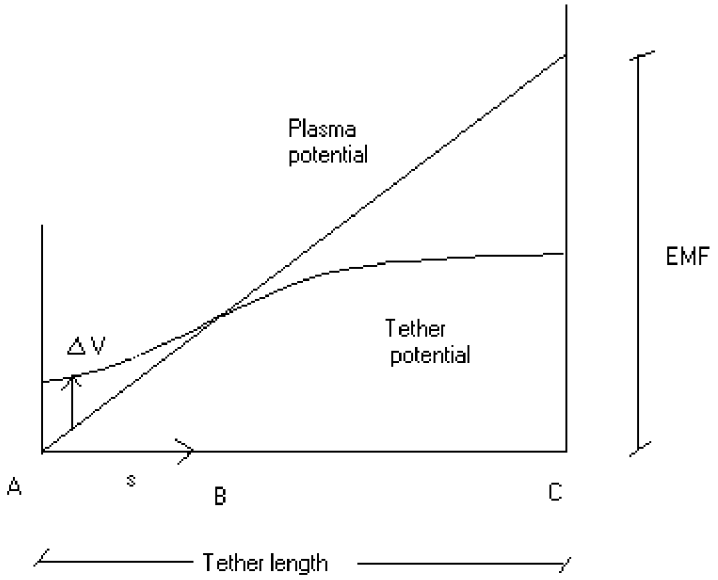

Figure 7